Int. J. Electrochem. Sci., 11 **(2016)** 4497 – 4514, doi: 10.20964/2016.06.79

International Journal of
ELECTROCHEMICAL
SCIENCE
www.electrochemsci.org

Electrochemical Techniques for Hydrocarbon Leak Detection in Cooling Water Systems

A.S. Pelliccione[*], *A.B. da Silva, E.A. de Souza, J.A.C.P. Gomes*

[1] Rua Ulysses Guimarães, 565, Rio de Janeiro, RJ, Brazil
[2] Avenida Horácio Macedo, 2030, Bloco I, Cidade Universitária, Centro de Tecnologia, Rio de Janeiro, Brazil
[*]E-mail: andre.pelliccione@petrobras.com.br

Received: 2 March 2016 / *Accepted:* 18 April 2016 / *Published:* 4 May 2016

Open recirculating cooling water systems are commonly used in petroleum industries, mainly in oil refineries. Heat exchangers are often applied to cool or condense process fluids. The chemical treatment used in cooling water system is essential to prevent corrosion, scaling, fouling and microbiological growth. When tubes fail due to corrosion, the cooling water can be contaminated with hydrocarbons. This contamination may cause corrosion, fouling and microbiological growth. The main purpose of this study is to evaluate electrochemical techniques for quick detection of hydrocarbon leaks in cooling water systems. To this purpose, synthetic cooling water with and without inhibitors, dispersant and biocide was prepared, based on the historical parameters of a refinery cooling water system. Diesel was injected in order to simulate hydrocarbon leak. The electrochemical tests were carried out on carbon steel and brass electrodes that are materials commonly used in heat exchangers of cooling water systems. The results showed that electrochemical impedance spectroscopy and linear polarization resistance tests carried out on brass electrodes were able to detect diesel leak in synthetic cooling water.

Keywords: cooling water, hydrocarbon, diesel, leak, electrochemical techniques

1. INTRODUCTION

Open recirculating cooling water system is a vital unit of a petroleum refinery. Problems affecting the performance of this system are corrosion, scale formation and biofouling [1].

Corrosion depends on the water parameters and on the materials used. Scale is caused by precipitation of compounds that become insoluble at higher temperatures, such as calcium carbonate and interferes with heat transfer and flow. Fouling results from the settling out of suspended solids,

build-up of corrosion products and growth of microbial masses bringing together corrosion under deposits [2-4]. Corrosion, scaling and fouling scarcely occur independently and are usually caused with a mutual relationship. A suitable chemical treatment program must be applied to prevent or control corrosion and deposition processes, according to the make-up and cooling water qualities [5]. Inhibitors, dispersants and microbiocides are added to cooling water systems to control corrosion, scaling, particulate fouling and microbiological activity. Orthophosphate and polyphosphate salts, organic phosphorous compounds (e.g., phosphonates), molybdate, zinc salts, copper inhibitors (e.g., azoles) are examples of common corrosion inhibitor. Scales inhibitors and dispersants include organic phosphorous compounds, polymers, copolymers and complex polymers [4]. To control the growth of bacteria, fungi, algae and protozoa, programs employing oxidizing microbicides, nonoxidizing microbicides, and biodispersants are often used [6]. Chlorine is a powerful oxidizing agent and one of the most versatile chemicals used in water treatment [7]. Another significant aspect of the cooling water quality monitoring is the detection and correction of leakage of process fluids or other contaminants. Hydrocarbon leaks in cooling water systems adversely affect equipment performance and operating costs. Therefore, quick determination of the source of a leak is required. Unfortunately, determining the source of hydrocarbon leaks in cooling system can be a long and tedious process. Efforts to improve the simplicity of this process and reduce detection time have a significant effect on plant performance and operating profits. A hydrocarbon process leak in a cooling water system promote microbiological growth, because hydrocarbon acts as a food source for naturally existing microbiological life forms (algae, fungi and bacteria) present in a cooling tower. The main problem of microbiological growth in cooling water systems is fouling, which can lead to corrosion of metal surfaces (by physical deposition, production of corrosive byproducts and depolarization of the corrosion cell caused by chemical reactions) and reduction the performance of heat exchangers by limiting heat transfer. In addition to microbiologically induced corrosion, a hydrocarbon leak may also cause corrosion in cooling water system, because deposit formation on metal surface caused by hydrocarbon build up can prevent corrosion inhibitors from reaching and passivating fouled surfaces; and because increased amounts of chlorine are fed to control and minimize increased microbiological activity, increasing chloride ion concentration and affecting directly copper and copper alloys [8]. If process contamination is a recurring problem, specific manual or automatic analytical assays are often used. For rapid detection of volatile hydrocarbon leaks, an appropriate analyzer is often installed on the return water. Heavier water-soluble hydrocarbons are usually detected by an online total organic carbon analyzer, an online gas chromatograph designed for a specific component, or an online measurement of oxidation-reduction potential (ORP). When online analyzers are not available, manual methods are used. For hydrocarbons that remain at least partially soluble in water, gas chromatography or mass spectrometer is often used. For hydrocarbons that are insoluble in water, an oil and grease analysis can be performed. When several potential leak sources exist, the extracted oil is usually analyzed by gas chromatography or true boiling point analysis to identify the leaking stream. For volatile hydrocarbons or industrial gases, the sample is typically analyzed by the purge and trap gas chromatography method [4]. Activate carbon filter and gas trap can be used to recover heavy hydrocarbons and collect light hydrocarbons from contaminated cooling water for gas chromatography analysis [8].

A study [9] demonstrated that localized corrosion monitoring (LCM) technique appears to be able to detect hydrocarbon leak (overhead gases from a column containing H_2S, CH_4, C_3H_8, C_4H_{10}, etc.) about seven to nine days before confirmation. The LCM detected the leak probably due to increase in microbial activities associated with the early stage of leak [9]. After a gas oil leak, the LCM was able to provide a warning on the heat exchanger failure with the sudden increase in localized corrosion rate two to three days before LPR responded and more than two weeks before being confirmed by other methods (cooling tower hydrocarbon foaming) [9,10]. This localized corrosion monitor is based on a differential flow technique and performs on-line real time measurements of localized corrosion rate (e.g., pitting, crevice and under deposit corrosion). The instrument part of LCM contains a solution resistance-compensated corrosion rate monitor based on the linear polarization resistance (LPR) technique, a zero-resistance ammeter (ZRA), a relay, an analog/digital (A/D) input/output acquisition and control board, and a personal computer. The localized corrosion rate obtained by this technique is based on ZRA and LPR readings [10, 11].

The main aim of this study is to evaluate electrochemical techniques for quick detection of hydrocarbons in cooling water systems, even in absence of contaminants in hydrocarbon (e.g., hydrogen sulfide, ammonium) and also without microbial activities, in order to identify quickly the leak and act to minimize damages to the cooling water treatment.

To this purpose, linear resistance polarization (LPR) and electrochemical impedance spectroscopy (EIS) tests were carried out on a corrosion loop, using working electrodes manufactured from carbon steel tube ASTM A179 [12] and aluminum brass tube ASTM B111 UNS C68700 [13] that are commonly materials used in heat exchanger tubes in petroleum refineries. The tests were conducted on a solution based on the historical parameters of an oil refinery cooling water system. Diesel was injected to simulate hydrocarbon leaks in cooling water.

2. EXPERIMENTAL

2.1 Test solutions

Table 1. Upper limit, lower limit, average measured between 2012 and 2015 of the main parameters in an oil refinery cooling water system and established parameters (ppm) for preparing synthetic cooling water.

Parameter	pH	Turbidity	Alkalinity	Calcium hardness	Total Hardness	Chloride	Sulfate	Conductivity	Total iron
Upper limit	7	0	50	0	0	0	0	0	0
Lower limit	8	60	250	700	900	1000	0	5000	5
Average 2012-2015	7.5	17.9	74.3	261.7	310.0	986.9	295.5	3968.7	0.4
Established parameters	7.5	X	80	270	320	1000	300	x	x

Three solutions were used in the tests: baseline water (BW); treated water (TW) and diesel contaminated water (DCW). The testing solutions were prepared in order to reproduce the average values of the main parameters of critical cooling water from an oil refinery measured between 2012 and 2015, as indicated in Table 1.

2.1.1 Baseline Water (BW)

The baseline water was prepared using calcium chloride to adjust calcium hardness, magnesium chloride to adjust magnesium hardness, sodium chloride to adjust chloride, sodium bicarbonate to adjust total alkalinity and sodium sulfate to adjust sulfate. The conductivity of the solution was measured and the values ranged between 3150 and 3900 $\mu S.cm^{-1}$, close to the average historical values. Titration was performed to measure chloride (957.4 $mg.L^{-1}$) and hardness (241.2 $mg.L^{-1}$ calcium hardness and 46.0 $mg.L^{-1}$ magnesium hardness), being coherent with the historical values.

2.1.2 Treated Water (TW)

For preparation of the TW, corrosion inhibitors for carbon steel and brass were added together with dispersant, as shown in Table 2. The ranges of active corrosion inhibitors and dispersant were defined based on historical parameters of the refinery cooling water and determined through the WaterCycle® Rx simulation software.

Table 2. Corrosion inhibitors and dispersant used to prepare the TW.

Chemical	Active (ppm)	Percent in solution	Dosage (ppm)
Hexametaphosphate	9.5	20%	47.5
Zinc chloride	2.5	24%	10.4
Tolyltriazole	3.5	45-55%	7
Dispersant – terpolymer	32.5	50%	65

2.1.3 Diesel contaminated water (DCW)

To simulate hydrocarbon leak, 20 $mL.L^{-1}$ of diesel S10 (containing less than 10 $mg.Kg^{-1}$ of sulfur) was added in treated water (TW). This is the concentration limit established for early contingency plan (20 ppm of oil and grease), based on existing empirical knowledge.

2.1.4 Biocide dosage

For the TW and DCW, it was also dosed biocide, by using diluted sodium hypochlorite (15:1). The flow rate was controlled by a manual valve, aiming to maintain free chlorine residual within the

target control range (0.3 and 0.5 ppm). The free chlorine measurement was performed with a portable photometer.

2.3 Materials

Working electrodes for the electrochemical tests were prepared from seamless heat exchangers tubes (¾ inch outside diameter) of carbon steel in accordance with ASTM A179 and aluminum brass in accordance with ASTM B111 UNS C68700.

The chemical compositions of these materials were analyzed by spark emission spectrometry using the Foundry-Master Pro equipment manufactured from Oxford Instruments.

2.4 Corrosion loop and electrochemical tests

The tests were carried out at the same time in two similar corrosion loops, of which one was designed to test carbon steel electrodes and other to test brass electrodes. Each loop was composed by polypropylene (PP) tank, chlorinated polyvinyl chloride (CPVC) pipes, centrifugal pump, electrical resistance, thermostat, temperature controller and flowmeter, as shown in Figures 1 and 2. The installation locations of corrosion coupons are indicated by red circles shown in Figure 1. The flow direction is indicated by arrows shown in Figure 2.

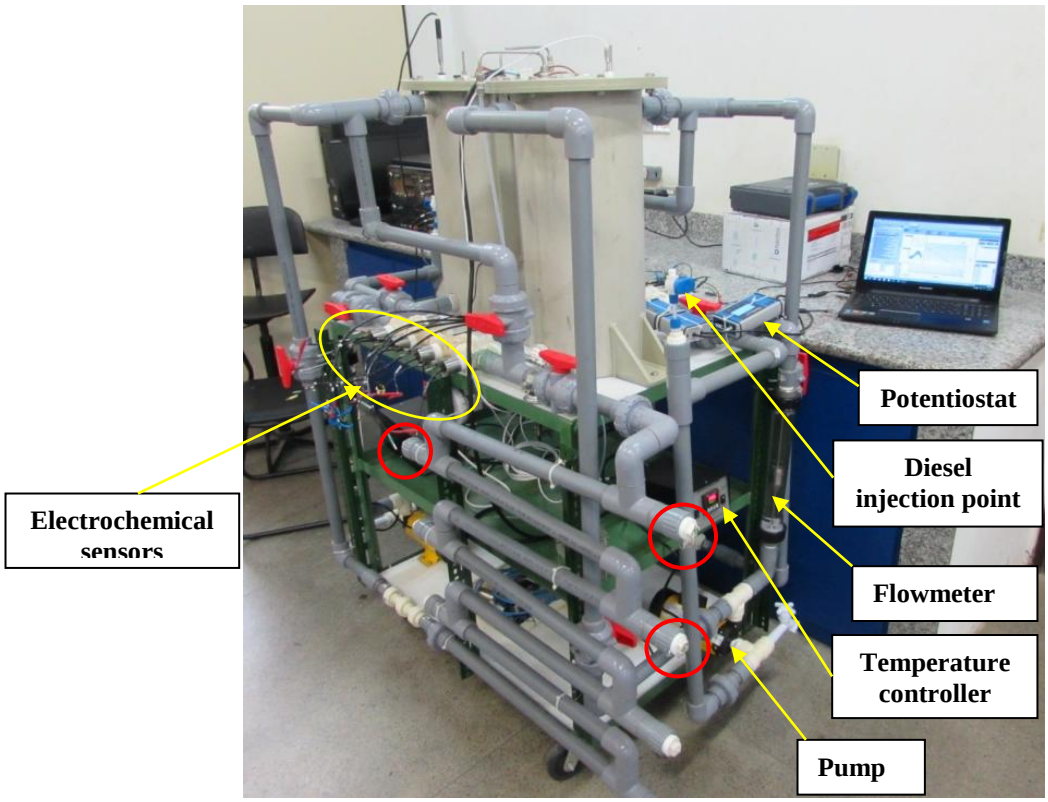

Figure 1. Corrosion loops used for the tests. The installation locations of corrosion coupons are indicated by red circles.

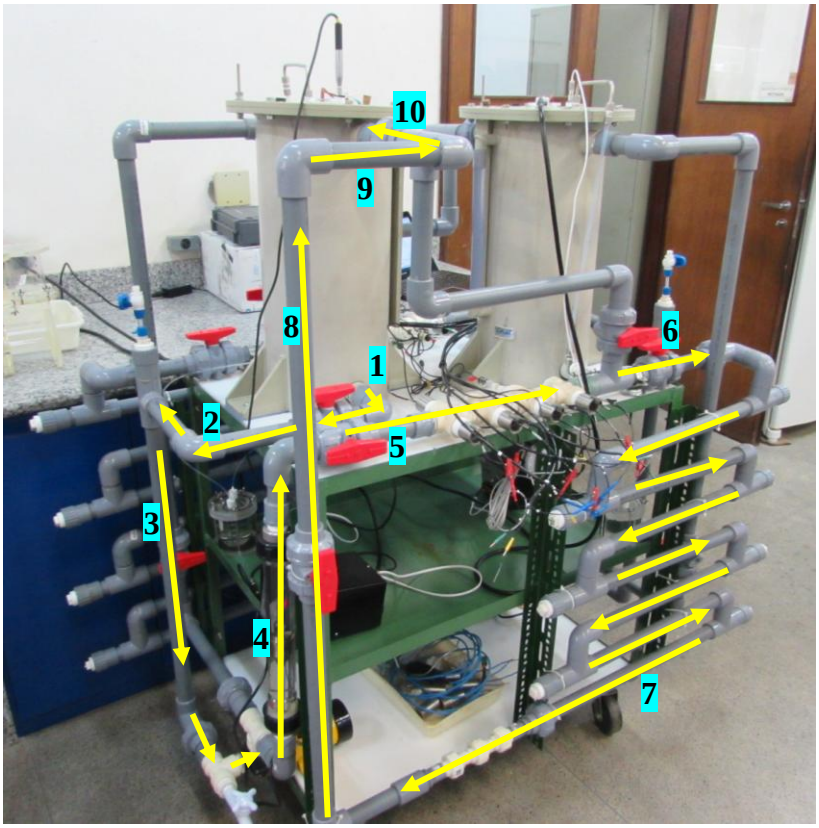

Figure 2. Corrosion loops used for the tests. The flow direction is indicated by arrows and numbers.

For each round of testing was used 25 L of solution. The measured flow rate was 1,9 $m^3.h^{-1}$, resulting in 1 $m.s^{-1}$ water velocity, that is consistent with recommended water velocity ranges for carbon steel and brass in cooling water systems pipes.

All tests were performed at 40 °C +/- 1 °C based on the typical temperature of the water that returns to the cooling tower. Working electrodes manufactured from carbon steel and brass tubes were mounted in a stainless steel pipe (counter electrode) and fitted in series to the pipe of corrosion loop. A saturated calomel reference electrode was fitted to the pipe near to the working electrodes. Before the tests, the working electrodes were wet ground to grit 600, cleaned with distilled water and ethanol, and dried under airflow. The exposed area was 0.83 cm^2 for carbon steel and 0.62 cm^2 for aluminum brass. For linear polarization resistance (LPR), the curves were obtained from polarization of the electrode over a range of +/- 10 mV in relation to the open circuit potential (OCP), with a scan rate of 20 $mV.min^{-1}$. The polarization resistance (Rp) was obtained by the slope of the tendency line generated by linear regression for each curve. It was also carried out anodic polarization test from OCP to 500 mV above the OCP, with a scan rate of 20 $mV.min^{-1}$; and cathodic polarization test from OCP to 200 mV below the OCP, with a scan rate of 20 $mV.min^{-1}$.

The electrochemical Impedance Spectroscopy (EIS) measurements were performed at the open circuit potential (OCP) in the 10000 to 0.01 Hz frequency range and 50 points were recorded. A multichannel Palmsens® 3 potentiostat and a computer with PSTrace 4.7 software were used to

perform the electrochemical tests. For each corrosion loop, one channel of potentiostat was applied to LPR test and another channel to EIS test. Because these are non-destructive techniques, the electrochemical data acquisition could be performed at different times. After reaching 40 °C, the measurements of Rp and EIS parameters were carried out at 2, 14, 28, 42, 56 and 68 hours. For DCW without and with sodium hypochlorite, diesel was injected after 21 hours. Therefore the first measurement of OCP and Rp with diesel in solution was performed at 28 hours (7 hours after diesel injection).

In order to verify short term changes in electrochemical parameters after diesel injection and the possible interference of sodium hypochlorite dosage in the results, there were performed LPR and EIS tests at 1, 2, 4, 8 and 16 hours. Then, sodium hypochlorite was dosed and new readings were carried out at 1, 2, 4, 6, 10, 14, 18 and 22 hours. After this, diesel was added at the solution and new readings were performed at 1, 2, 4, 6, 8, 10, 14, 18 and 22 hours.

The pH of solutions were measured at the beginning and every 12 hours of test and the values varied between 7 and 8, which is consistent with the historical values shown in Table 1.

2.5 Mass loss measurements

Triplicate rectangular specimens of carbon steel (manufactured from ASTM A179 tube) and brass (manufactured from ASTM B111 C68700 tube) were immersed in their respective corrosion loop and mass loss measurements were performed after 72 hours in BW, TW, DCW, TW with sodium hypochlorite and DCW with sodium hypochlorite. The installation location and positioning of corrosion coupons are indicated in Figures 1 and 3. Preparing, cleaning and evaluating procedure were carried out according ASTM G1-03 [14]. The main purpose of this test was to verify the effect of sodium hypochlorite dosage and diesel addition on corrosion rate of carbon steel and brass.

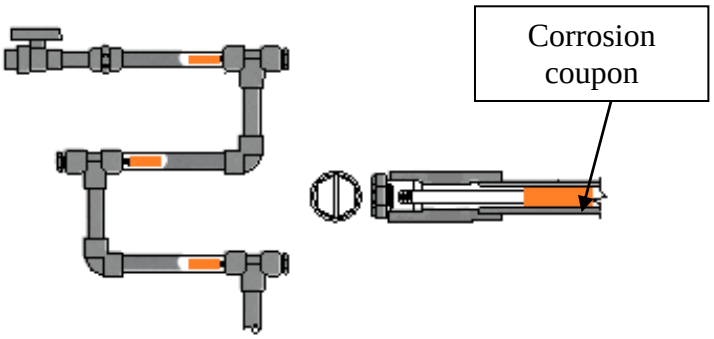

Figure 3. Installation of corrosion coupon

3. RESULTS AND DISCUSSION

3.1 Chemical composition

The three readings of main elements for carbon steel and brass detected by optical emission spectrometry were coherent with ASTM standards, according Table 3.

Table 3. Results of chemical analysis

Element	Tube material	ASTM A179	Element	Tube material	ASTM B111 C68700
Iron	99,0	Remainder	Copper	78,4	76,0 – 79,0
Carbon	0,09	0,06 – 0,18	Zinc	19,1	Remainder
Manganese	0,46	0,27 – 0,63	Aluminum	2,1	1,8 – 2,5
Sulphur	0,005	0,035 max.	Lead	0,01	0,07 max.
Phosphor	0,007	0,035 max.	Arsenic	0,02	0,02 – 0,06
Silicon	0,21	--	Iron	0,05	0,06 max.

3.2 Electrochemical tests

3.2.1 Carbon steel

The open circuit potential (OCP) and polarization resistance (Rp) versus time measured in BW, TW, DCW, TW with sodium hypochlorite dosage and DCW with sodium hypochlorite dosage are shown in Table 4.

From this table, it can be seen that the OCP tends to stabilize after 28 hours for all test solutions. The OCP was lower in BW than the other test solutions and the Rp values were significantly lower in BW than TW. These results indicate positive effect of corrosion inhibitors for carbon steel in reducing the corrosion rate. There were no significant changes in Rp values caused by diesel injection in DCW with and without sodium hypochlorite dosage.

Table 4. OCP (mV_{SCE}) and Rp ($ohm.cm^2$) versus time (hours) for tests carried out on carbon steel.

Time	BW		TW		DCW[1]		TW with hypochlorite			DCW with hypochlorite[1]		
	OCP	Rp	OCP	Rp	OCP	Rp	OCP	Rp	Free chlorine residual	OCP	Rp	Free chlorine residual
2	-680	0,2	-564	4,6	-585	3,8	-563	25,2	0,7	-529	12,1	0,8
14	-701	0,4	-574	7,2	-633	5,6	-593	10,6	0,3	-580	10,8	1,2
28	-700	0,4	-596	5,5	-582	6,5	-622	11,4	0,7	-637	7,7	0,5
42	-695	0,5	-595	6,0	-582	6,6	-638	13,8	0,3	-620	6,3	0,5
56	-693	0,5	-592	6,0	-579	6,4	-646	16,1	0,9	-635	6,4	0,5
68	-690	0,5	-600	6,3	-579	5,9	-656	17,9	0,8	-629	5,8	0,3

[1] Diesel addition after 15 hours.

The results of OCP and Rp versus time for the tests that aimed to verify short term changes after diesel addition in the water are shown in Table 5. It was not verified significant changes in Rp after sodium hypochlorite dosage. There were no significant changes in Rp after diesel addition, as also observed in previous tests (Table 4), implying that LPR measurements in carbon steel are not a satisfactory technique for diesel leak detection in cooling water system.

Table 5. OCP (mV_{SCE}) and Rp ($ohm.cm^2$) versus time for tests carried out on carbon steel and brass, aiming to verify short term changes.

Carbon Steel				Brass		
Time	OCP	Rp	Free chlorine residual	OCP	Rp	Free chlorine residual
1	-562	7,97	N/A	-99	117,0	N/A
2	-560	9,71	N/A	-84	129,8	N/A
4	-553	10,10	N/A	-63	135,2	N/A
8	-557	11,14	N/A	-69	75,1	N/A
16	-598	21,22	N/A	-65	96,0	N/A
After hypochlorite dosage				After hypochlorite dosage		
1	-596	23,5	0,73	-63	41,4	0,77
2	-598	23,7	0,79	-68	42,8	0,60
4	-602	23,1	0,57	-74	59,5	0,36
6	-608	19,7	0,48	-56	29,9	0,30
10	-610	19,1	0,33	-71	7,3	0,60
14	-619	21,5	between 0,33 and 0,62	-71	8,7	between 0,60 and 0,43
18	-622	22,2	between 0,33 and 0,62	-76	15,8	between 0,60 and 0,43
20	-624	19,3	between 0,33 and 0,62	-86	34,5	between 0,60 and 0,43
22	-625	21,3	0,62	-102	42,4	0,43
After diesel addition				After diesel addition		
1	-625	21,1	0,82	-79	40,8	0,56
2	-625	22,7	0,83	-72	23,2	0,80
4	-625	20,1	0,84	-64	34,4	1,21
6	-625	21,5	0,60	-74	41,8	0,96
8	-625	22,0	0,75	-81	54,1	0,90
10	-627	21,9	between 0,75 and 0,05	-90	75,2	between 0,90 and 0,10
14	-629	22,1	between 0,75 and 0,05	-112	110,0	between 0,90 and 0,10
18	-631	22,7	between 0,75 and 0,05	-138	141,3	between 0,90 and 0,10
22	-635	23,6	0,05	-148	150,9	0,10

The shape of Nyquist plots showed a capacitive behaviour for all tests. The tests performed at 2, 14, 28, 42, 56 and 68 hours are shown in Figures 4 and 5. Comparing BW with the other solutions, it can be observed lower values of Rp, based on extrapolation of capacitive arcs, indicating the beneficial effect of corrosion inhibitors for carbon steel electrode.

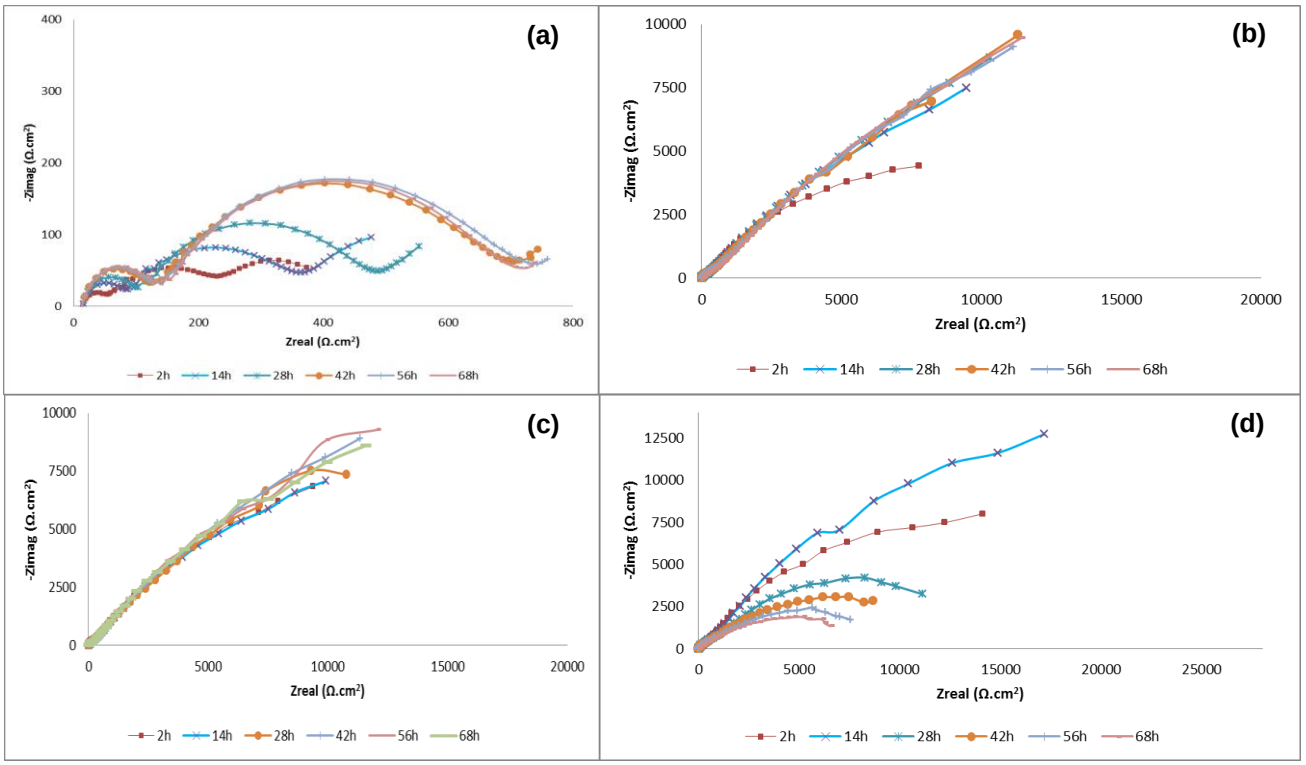

Figure 4. Nyquist plot obtained at corrosion potential for carbon steel. (a) Baseline water (BW). (b) Treated water (TW). (c) Diesel contaminated water (DCW). (d) Treated water (TW) with sodium hypochlorite dosage.

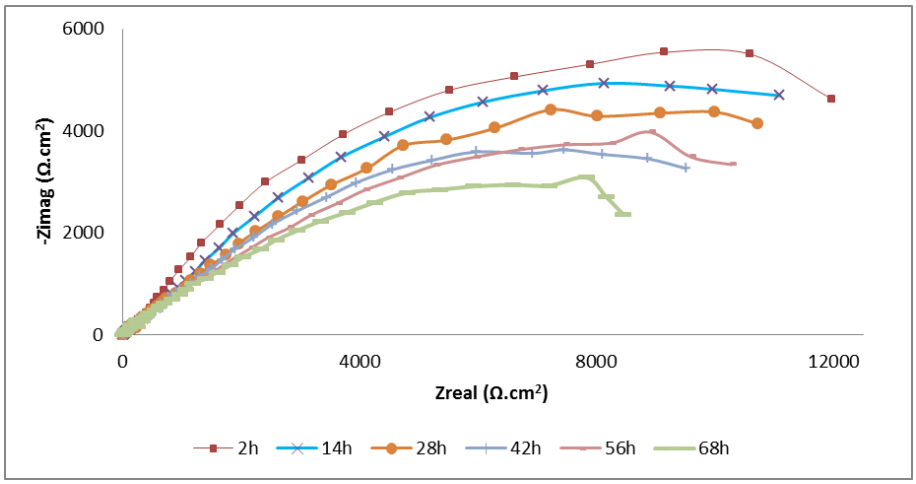

Figure 5. Nyquist plot obtained at corrosion potential for diesel contaminated water (DCW) with sodium hypochlorite dosage. Diesel was injected after 20 hours.

Electrochemical impedance spectroscopy measurements performed in short intervals of time are shown in Figures 6 and 7.

The variations between the diameters of capacitive arcs before sodium hypochlorite dosage, after sodium hypochlorite dosage and after diesel addition were not significant, indicating that sodium hypochlorite dosage and diesel addition did not promote significant changes in EIS results.

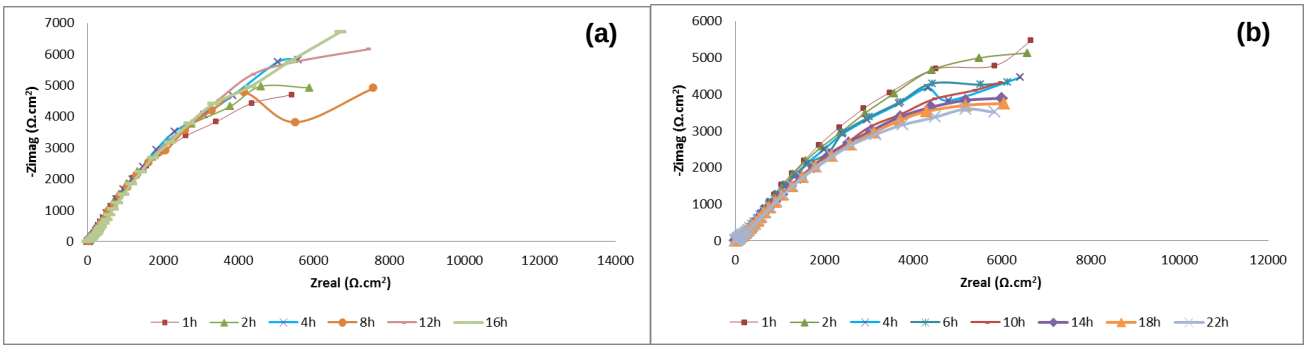

Figure 6. Nyquist plot obtained at corrosion potential for carbon steel. (a) Treated water (TW). (b) Second part of the test after sodium hypochlorite dosage.

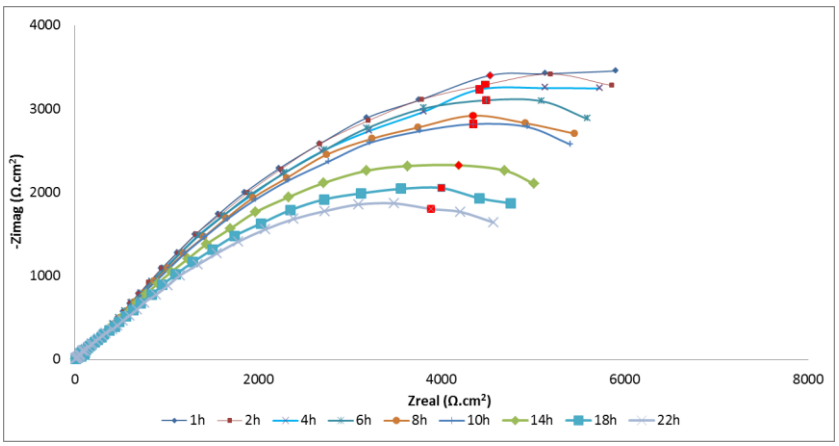

Figure 7. Final part of the test after diesel addition. Impedance measurements at 0,02 Hz are indicated by red points.

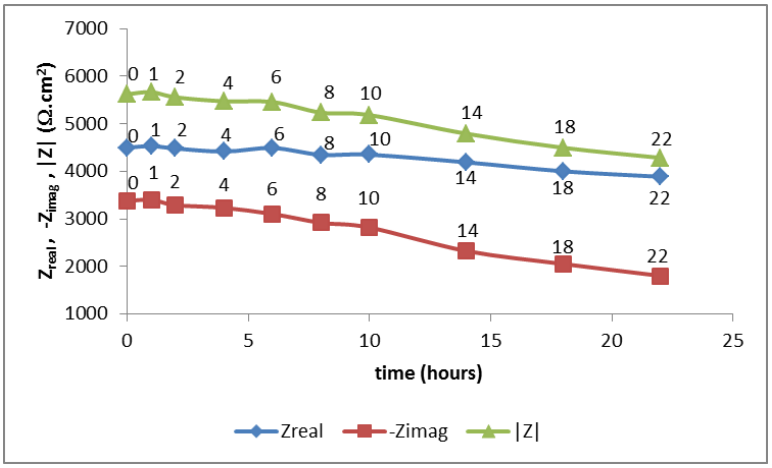

Figure 8. Z_{real}, $-Z_{imag}$ and |Z| versus time after diesel injection for carbon steel.

It was found that the major differences between impedance values (in the same frequency) obtained from Nyquist diagrams plotted at different times occurred at 0,02 Hz, as indicated in Figure 7.

Based on this, the obtained values of real part, imaginary part and modulus of impedance versus time at 0,02 Hz were plotted, according to Figure 8. Time zero corresponds to the last test performed with sodium hypochlorite dosage (22 hours) and subsequent times correspond to tests with diesel addition. There were no significant changes between impedances, as shown in Figure 8. These results suggest that EIS carried out on carbon steel electrodes is not a satisfactory electrochemical technique for diesel leak detection in cooling water system.

Anodic and cathodic polarization curves are indicated in Figure 9. It was found that active dissolution was present throughout the entire tests, as shown with increase in current density.

It was observed that open circuit potential (OCP) of TW was about 80 mV higher than OCP of BW. The highest cathodic and anodic currents occurred in BW. These results show the beneficial effect of corrosion inhibitors for carbon steel electrode.

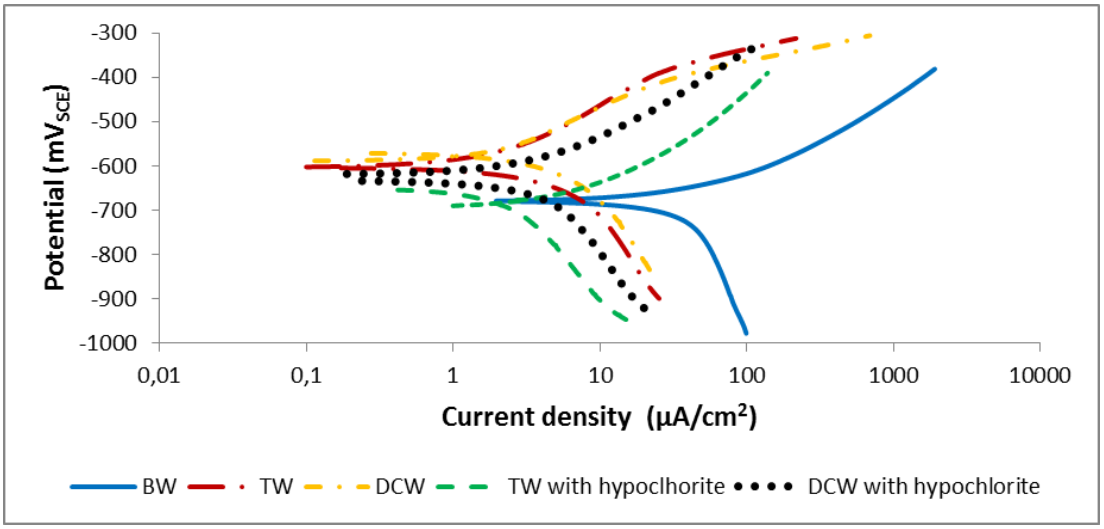

Figure 9. Cathodic and anodic polarization curves for carbon steel.

3.2.2 Brass

The open circuit potential (OCP) and polarization resistance (Rp) versus time measured in BW, TW, DCW, TW with sodium hypochlorite dosage and DCW with sodium hypochlorite dosage are shown in Table 6. The Rp values in TW with and without sodium hypochlorite dosage were significantly higher than in BW. These results indicate good performance of corrosion inhibitor for brass (tolyltriazole) in reducing the corrosion rate, even without hypochlorite dosage. There was a significant increase of Rp at 28 hours in DCW with sodium hypochlorite dosage, that is, after the diesel injection. However, in TW with sodium hypochlorite dosage it was also found that Rp reached similar values at 42 hours. However it was not possible to determine the influence of diesel in the change of Rp for testing intervals indicated in Table 6.

Table 6. OCP (mV_{SCE}) and Rp ($ohm.cm^2$) versus time (hours) for tests carried out on brass.

Time (hours)	BW		TW		DCW[1]		TW with hypochlorite			DCW with hypochlorite[1]		
	OCP	Rp	OCP	Rp	OCP	Rp	OCP	Rp	Free chlorine residual	OCP	Rp	Free chlorine residual
2	-128	13,26	-40	107,68	-136	80,52	-32	13,33	0,6	-25	10,77	1,0
14	-20	25,38	-26	72,59	-37	100,30	-70	86,44	0,3	-38	83,76	1,0
28	-40	21,69	-30	77,38	-22	71,26	-48	65,04	0,9	-101	219,13	0,9
42	-50	18,68	-30	115,63	-20	59,85	-105	279,56	0,3	-141	290,40	0,8
56	-60	22,25	-32	95,50	-26	51,07	-104	227,57	0,4	-147	325,06	0,5
68	-62	24,48	-54	127,28	-23	49,59	-130	235,44	0,5	-158	381,08	0,4

[1] Diesel addition after 15 hours.

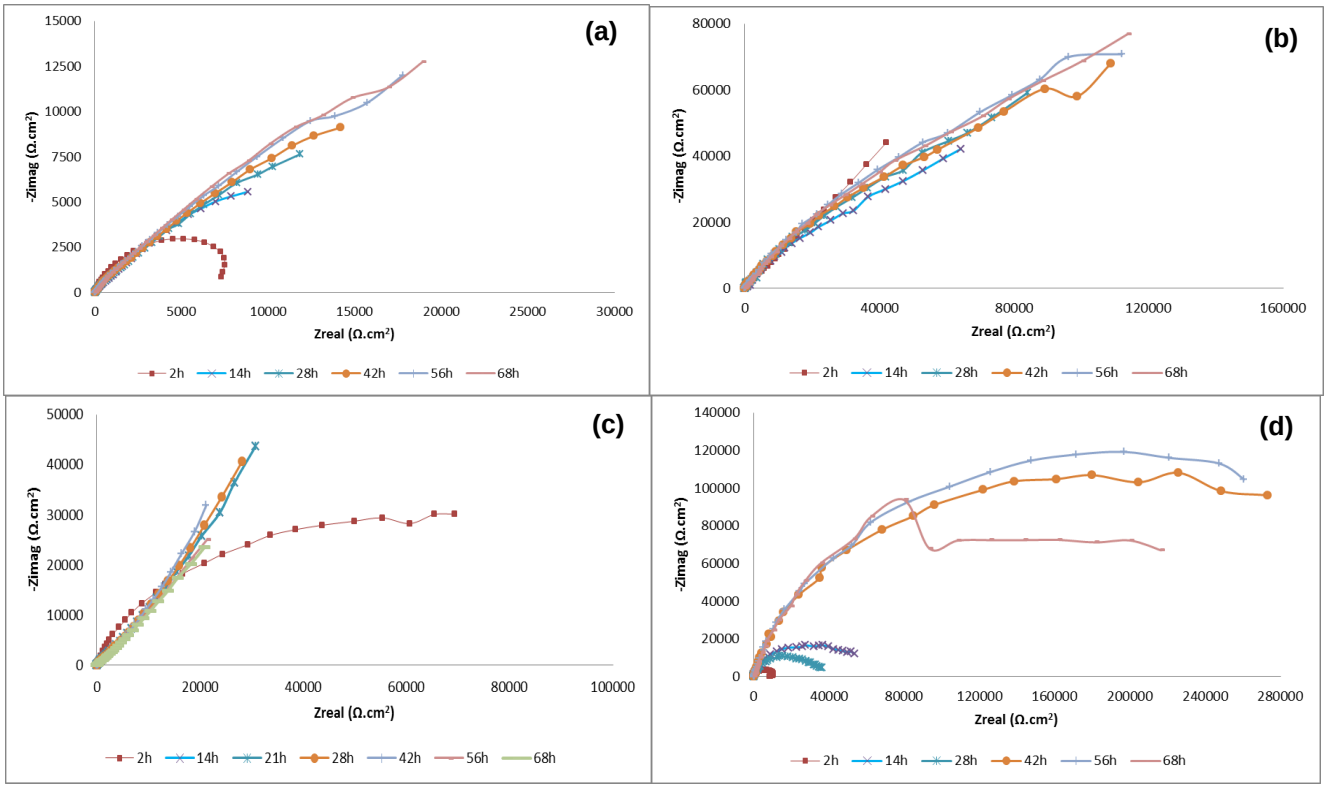

Figure 10. Nyquist plot obtained at corrosion potential for brass. (a) Baseline water (BW). (b) Treated water (TW). (c) Diesel contaminated water (DCW). (d) Treated water (TW) with sodium hypochlorite dosage.

The results of OCP and Rp versus time for the tests that aimed to verify short term changes after diesel addition in the water are indicated in Table 5. Sodium hypochlorite dosage led to Rp reduction, suggesting disrupt of triazole based corrosion inhibitor by sodium hypochlorite. According to Huynh [15], chlorine, as made available by the hypochlorite ion, may disrupt the triazole inhibitor film if applied in sufficient concentration and for extend exposure times, resulting in a loss of copper

surface protection. At the same time, chlorine reacts with BZT (benzotriazole) or TTA (tolyltriazole) in the bulk water and drastically reduces its ability to form new inhibitor film [16].

Still according to Table 5, after sodium hypochlorite dosage and before diesel injection, Rp have varied, but at 22 hours it tended to stabilize near to 40 ohm.cm2. After diesel injection, a reduction in Rp was observed at 2 hours, but at 4 hours it reverts to increase continuously, until the end of the test. This Rp reduction suggests that LPR carried out on brass electrode is a potential electrochemical technique to detect diesel leak in cooling water system.

The shape of Nyquist plots showed a capacitive behaviour for all tests. For tests conducted at 2, 14, 21, 28, 42, 56 and 68 hours, according to Figures 10 and 11, tendency of increasing in diameter of capacitive arcs (and consequently Rp increasing) was observed. In the TW with sodium hypochlorite dosage and DCW with sodium hypochlorite dosage, stabilization (similar capacitive arc diameter) was observed from 42 hours test.

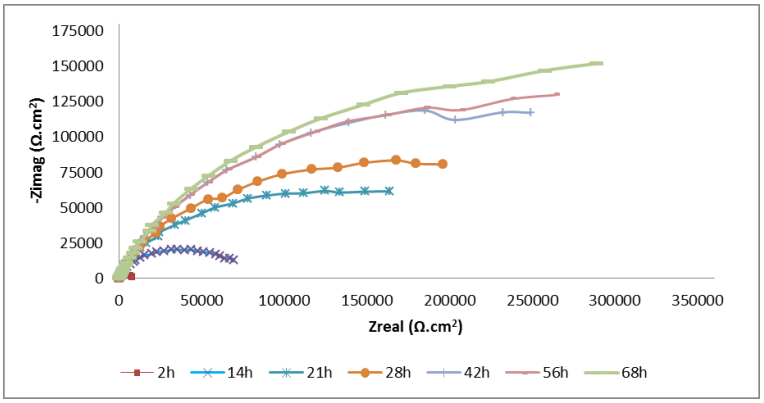

Figure 11. Nyquist plot obtained at corrosion potential for brass in diesel contaminated water (DCW) with sodium hypochlorite dosage. Diesel was injected after 20 hours.

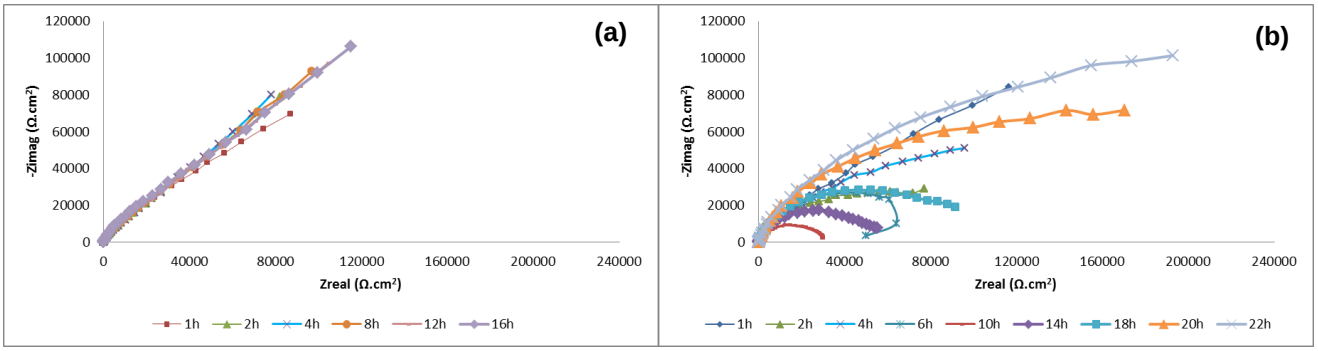

Figure 12. Nyquist plot obtained at corrosion potential for brass. (a) Treated water (TW). (b) Second part of the test after sodium hypochlorite dosage.

In the tests performed at short intervals of time as shown in Figures 12 to 14, there was rapid stabilization (similar capacitive arc diameter) in TW solution (Figure 12a). After hypochlorite dosage (Figure 12b) there were variations between capacitive arc diameters, with the smaller occurring at 10

hours. After this period, the capacitive arc diameters increased with time until the end of this part of the test. Then, after diesel injection (Figures 13 and 14), it was verified significant reduction of capacitive arc diameters up to 4 hours of testing, followed by increasing of capacitive arc diameters until the end of the test.

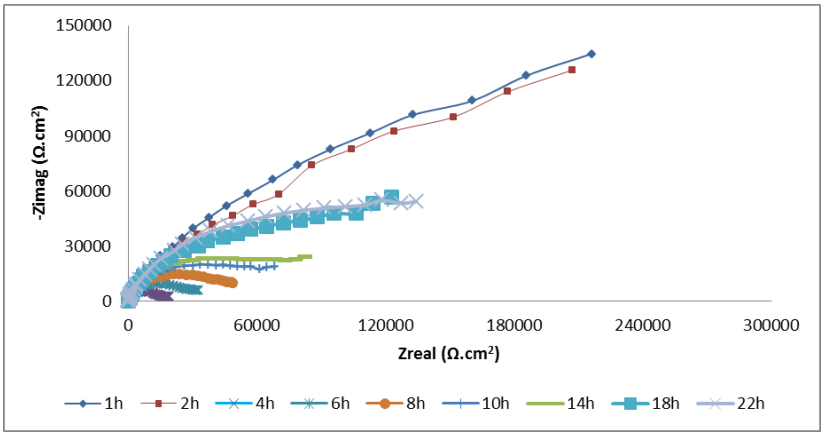

Figure 13. Final part of the test after diesel addition.

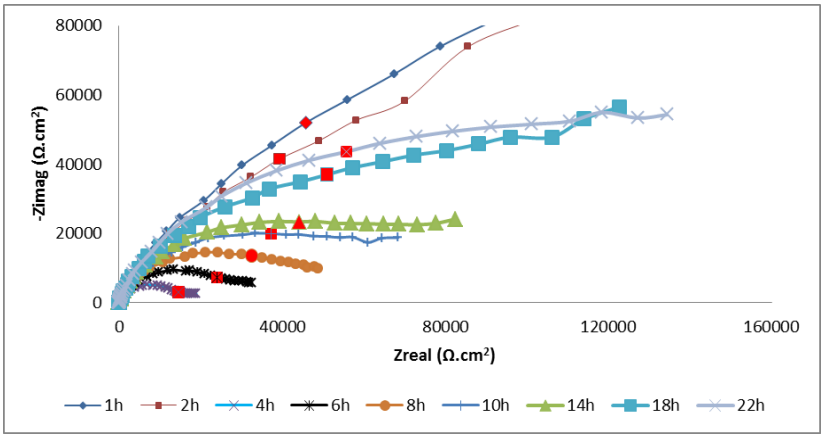

Figure 14. Same as previous plot, but on an expanded scale. Impedance measurements at 0,13 Hz are indicated by red points.

It was observed that the major differences between impedance values (in the same frequency) obtained from Nyquist diagrams plotted at different times occurred at 0,13 Hz, as shown in Figure 14.

Based on this, the obtained values of real part, imaginary part and modulus of impedance versus time at 0,13Hz were plotted, according to Figure 15. Time zero corresponds to the last test performed with sodium hypochlorite dosage (22 hours) and subsequent times correspond to tests with diesel addition. It can be observed significant reduction of impedances up to 4 hours, followed by increasing until the end of the test. Therefore, based on these results, there was a transient response after diesel addition detected by EIS tests. This transient response was also detected by LPR test. This evidence implies that EIS test carried out on brass electrode is a potential electrochemical technique

for diesel leak detection in cooling water systems. The reason for this transient response may be associated with the metal-electrolyte interface changes after diesel addition, probably due to diesel interaction with corrosion inhibitor on brass electrode surface.

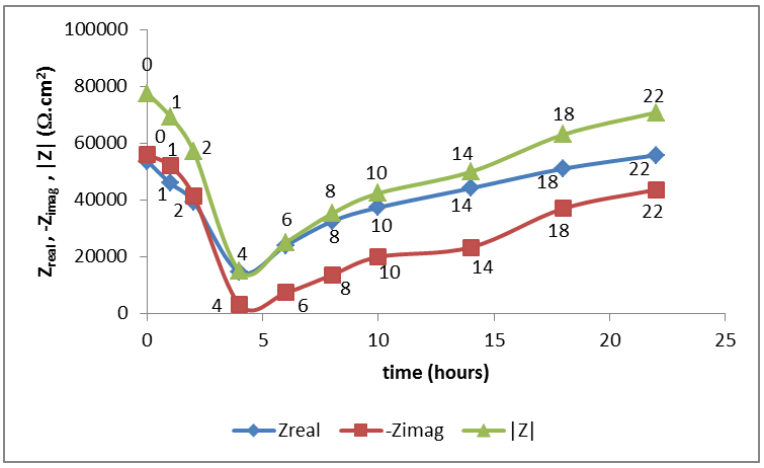

Figure 15. Z_{real}, $-Z_{imag}$ and |Z| versus time after diesel injection for brass.

Anodic and cathodic polarization curves are shown in Figure 16. It was found that active dissolution was present throughout the entire tests, as shown with increase in current density. It was verified that open circuit potential (OCP) of TW was about 10 mV higher than OCP of BW. The highest anodic currents occurred in BW, indicating the beneficial effect of corrosion inhibitor for brass electrode.

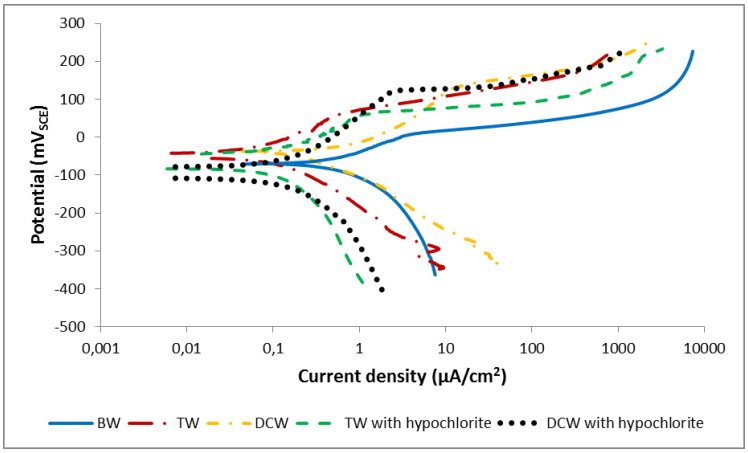

Figure 16. Cathodic and anodic polarization curves for brass in test solutions.

3.3 Mass loss test

The results of mass loss measurement are described in Table 7. The corrosion inhibitors show satisfactory efficiency for carbon steel and brass protection, as observed by reduction of corrosion rate in TW compared to BW.

The corrosion rate of carbon steel in DCW with hypochlorite dosage increased. The corrosion rate of brass in DCW without and with diesel dosage increased. These results suggest that diesel may be interfering with the inhibitor films formed on carbon steel and brass surface, favoring the increase of corrosion rate.

Table 7. Corrosion rates (mpy) for carbon steel and brass from the mass loss test.

Test solution	**Corrosion rate (mpy)**	
	Carbon steel	Brass
BW	20	1,9
TW	2	0,2
DCW	2	0,6
TW with hypochlorite	2	0,2
DCW with hypochlorite	3	0,6

4. CONCLUSIONS

- The corrosion inhibitors for carbon steel (hexametaphosphate and zinc chloride) and for brass (tolyltriazole) were effective in reducing the corrosion rate, as evidenced by results of linear polarization resistance (LPR), electrochemical impedance spectroscopy (EIS), cathodic and anodic polarization, and mass loss tests.
- The significant reduction of capacitive arc diameters, real part, imaginary part and modulus of impedance up to 4 hours followed by increasing until the end of the test indicates that EIS in brass electrode is a potential electrochemical technique for diesel and possible other hydrocarbons and contaminants leak detection in cooling water systems. This transient response in the metal-electrolyte interface after diesel addition is probably associated with diesel interaction with corrosion inhibitor on brass electrode surface. In addition, the largest variations between impedances occurred at 0.13 Hz. Therefore, impedance measurements at 0,13 Hz (e.g., lasting 7,7 seconds each) may be able to detect leakage of diesel and possibly other hydrocarbons and other contaminants in cooling water systems.
- The Rp reduction for brass electrode after 2 hours diesel injection suggests that LPR carried out on this material is also a potential technique to detect diesel leak in cooling water system.
- There were no significant changes in Rp and impedance values in carbon steel electrodes after diesel injection, implying that LPR and EIS were not satisfactory electrochemical techniques for diesel leak detection in synthetic cooling water system using carbon steel electrodes. In addition, the largest ranges between impedance tests for carbon steel electrode after diesel injection occurred at 0,02 Hz. Therefore, each impedance measurement would last 50 seconds, being more susceptible to suffer interferences and fluctuations from the cooling water system.
- Sodium hypochlorite dosage led to Rp reduction in brass electrode, probably due to disruption of triazole based corrosion inhibitor by sodium hypochlorite and reduction of its ability to form new inhibitor film due to chlorine reaction with tolyltriazole in the bulk water. For carbon steel

electrode, it was not verified significant change in Rp values after sodium hypochlorite dosage.

- Mass loss tests showed that diesel in cooling water tends to increase the corrosion rate of carbon steel and mainly the corrosion rate of brass.

ACKNOWLEDGEMENTS
The authors thanks to Alecir Zenaide de Oliveira, Alice Branquinho Martins, Cassius Mazzeu, Jefferson Rodrigues de Oliveira, Lyzia de Souza Santos, Marcelo Eurípedes Ferreira Napolião, Roberto Carlos de Lima Areas and Wellington Fernandes Motta, who provided direct or indirect support during the tests.

References

1. P.K. Gogoi, B. Barhai, *Indian Journal of Chemical Technology*, 17 (2010) 291-295;
2. F.N. Kemmer, *The Nalco Water Handbook*, McGraw-Hill, United States of America (1987);
3. B. Cottis, M. Graham, R.Lindsay, S. Lyon, T. Richardson, D. Scantlebury, H. Stott, *Shreir´s Corrosion, v.2*, Elsevier B.V. (2010);
4. NACE Item No. 24238, 2009: Monitoring and Adjustment of Cooling Water Treatment Operating Parameters;
5. T. Hosokawa, M. Iwasaki, H. Komatsubara, Y. Makino, K. Matsubara, H. Morinaga, H. Suzuki, T. Suzuki, S. Takeda, M. Takemura, H. Takenaka, *Kurita Handbook of Water Treatment*, Kurita Water Industries LTD, Tokyo (1999);
6. NACE International Publication 11206, Item No. 24230, 2006: Biocide Monitoring and Control in Cooling Towers;
7. Cooling Water System, in: General Electric Company, *Handbook of Industrial Water Treatment*, http://www.gewater.com/handbook/index.jsp., accessed: January, 2016;
8. C. Spurrel, A. M. Harris, presented at The *NACE Annual Conference 96*, *Corrosion 96*, Denver, Colorado, (1996) Paper No. 610;
9. B. Yang, presented at *NACE Annual Conference 99, Corrosion 99*, San Antonio, Texas (1999) Paper No. 307;
10. Y. Lietai, *Techniques for Corrosion Monitoring*, Woodhead Publishing Limited, Cambridge (2008);
11. B. Yang, *Corrosion*, 56 (2000) 743-756;
12. ASTM A179-90a, 2012: Standard Specification for Seamless Cold-Drawn Low-Carbon Steel Heat-Exchanger and Condenser Tubes;
13. ASTM B111-11, 2011: Standard Specification for Copper and Copper-Alloy Seamless Condenser Tubes and Ferrule Stock;
14. ASTM G1-03, 2011, Standard Practice for Preparing, Cleaning, and Evaluating Corrosion Test Specimens, 2011;
15. N. H. Huynh, Ph.D Thesis, QUT, Australia (2004);
16. L. Cheng, R. C. May, K. M. Given, presented at *NACE Annual Conference 99, Corrosion 99*, San Antonio, Texas (1999), Paper No 101.